Biological Activities and 3D QSAR Studies of a Series of *Delisea pulchra* (cf. *fimbriata*) Derived Natural Products

Anthony D. Wright,*,[†] Rocky de Nys,[‡] Cindy K. Angerhofer,[§] John M. Pezzuto,[||] and Marion Gurrath[⊥]

Australian Institute of Marine Science, PMB No. 3, Townsville MC, Qld 4810, Australia, School of Marine Biology and Aquaculture, James Cook University, Townsville, Qld 4811, Australia, Aveda Corporation, Minneapolis, Minnesota 55449, College of Pharmacy, Nursing, and Health Sciences, Purdue University, West Lafayette, Indiana 47907, and Institute for Pharmaceutical Chemistry, Heinrich-Heine University, Universitätsstrasse 1, D-40225 Düsseldorf, Germany

Twenty-five natural products, mainly halogenated furanones, isolated from the temperate red algae *Delisea pulchra* were investigated for their cytotoxic, antimicrobial, and antiplasmodial effects, their inhibition of the activity of the enzymes HIV-1-RT (HIV-1-reverse transcriptase), PKC (protein kinase C), and TK (tyrosine kinase), and their inhibition of the biosynthesis of IL-1 (interleukin-1). All were found to mediate a positive response in one or more of these test systems. In particular, compounds **9**, **11**, **12**, **14**, **16**, **17**, **19**, and **20** demonstrated cytotoxic activity in all of the assays they were tested in; compounds **11**, **12**, **17**, **19**, and **20** were also active in the majority of the anti-infective screens. In the antimalarial and tyrosine kinase assays, compounds **17**, **19**, and **20** were all active. Molecular modeling studies employing 3D QSAR with receptor modeling methodologies performed with 16 halogenated furanones generated a pharmacophore hypothesis consistent with the experimentally derived cytotoxicity data. This hypothesis is developed around an active molecule having a framework based on compound **11** with an OH function or OAc (assay dependent) at C-7 and bulky electron-rich groups at C-6, such as Cl and Br but not I.

Delisea pulchra (cf. *fimbriata*)[1] (Greville) Montage (Bonnemaisonales, Bonnemaisoniaceae) is a common subtidal red alga in South Eastern Australia. It has been the focus of early pharmacological studies based on its strong antimicrobial activity.[2] *D. pulchra* produces a series of halogenated furanones[3−5] that play an important role in the ecology of the plant.[6,7] Furanones have strong feeding deterrent properties against generalist herbivores[7] and are bioaccumulated by more specialized predators, possibly as a chemical defense.[8] They are also natural antifouling agents located at the surface of the plant,[9] where they deter the settlement and growth of epiphytic bacteria[6] and macrofouling organisms.[10] Further studies based on the potent biological activity of furanones against epiphytic bacteria have led to the elucidation of the mechanism of action of these compounds in inhibiting the growth and biofilm development of Gram-negative bacteria. Furanones specifically interfere with the acylated homoserine lactone (AHL) genetic regulatory system that controls the expression of density-dependent phenotypes in many bacteria[11,12] and also affect the alternative autoinducer 2 (AI-2) signaling systems in both Gram-negative and Gram-positive bacteria.[13,14] They have been demonstrated to inhibit AHL regulated phenotypes in a diversity of bacteria including clinically important pathogens.[15,16]

While the natural products chemistry and function of furanones have been well studied, there is less information on the pharmacological activity of these compounds. The present study was undertaken to establish the potential of furanones as chemical leads that could be useful in the development of new therapeutic agents. To do this, a 3D QSAR molecular modeling study was performed with biologically active molecules to develop a pharmacophore hypothesis for cytotoxicity.

Results and Discussion

D. pulchra was collected from Cape Banks, New South Wales, Australia, and yielded 25 natural products, the majority of which

are halogenated furanones.[4,5] Biological testing of these compounds toward pharmacologically relevant targets was undertaken using in vitro bioassays. These studies targeted cytotoxic, antimicrobial, and antimalarial activities, enzyme inhibition for HIV-1-RT, PKC and TK, and the inhibition of IL-1 and protein biosynthesis. Compounds were limited in availability, and therefore not all compounds were used in all assays.

Evaluation of Cytotoxic Potential with Cultured Cancer Cell Lines. To determine the antineoplastic potential of the natural products, cytotoxic effects were evaluated with a battery of cultured tumor cells (Table 1). Of the 19 compounds that were tested (Table 1), 13 demonstrated ED_{50} values of ≤ 4 μg/mL in one or more human cancer cell test systems and were classified as active.[16] Compounds **11**, **12**, **14**, **16**, **17**, and **20** demonstrated the broadest spectrum of activity. Five compounds (**3**, **8**, **13**, **21**, and **25**) had weak activity ($20 \geq ED_{50} \geq 4$ μg/mL), while only one, an acyclic molecule (**23**), was completely inactive ($ED_{50} \geq 20$ μg/mL). Of the 13 active compounds, **11**, **14**, and **16** reversed vinblastine resistance in KB−V1 cells to some extent, demonstrating greater activity toward "drug-resistant" KB+V1 cells treated with vinblastine, compared to the cells without vinblastine treatment. Some selective cytotoxicity was also observed for compounds **13** and **21**. They were inactive toward the sensitive KB−V1 cells but moderately toxic toward human melanoma cells (Mel2).

Antimicrobial Activity. Furanones have strong antimicrobial activity; however, testing has been limited to the four major metabolites of *D. pulchra*.[2] A larger array of furanones and other metabolites from *D. pulchra* were tested using bioautographic assays that are efficient at detecting antimicrobial compounds.[18] Localization of activities on developed TLC plates is useful for testing crude extracts and directing isolation procedures. The current study employed a direct bioautographic technique with microorganisms grown directly on TLC plates.[19] Twenty-four compounds were evaluated using the fungus *Penicillium oxalicum*, the Gram-positive bacteria *Bacillus subtilis* and *Micrococcus luteus*, and the Gram-negative bacterium *Escherichia coli* as test organisms.

Furanones were significantly more active than the acyclic compounds (**22**−**24**) in all assays. There was a marked distinction between the antimicrobial effects of furanones against Grampositive and Gram-negative bacteria, with more compounds having

* To whom correspondence should be addressed. Tel: +61 7 4753 4204. E-mail: a.wright@aims.gov.au. Web site: www.aims.gov.au.
† Australian Institute for Marine Science.
‡ James Cook University.
§ Aveda Corporation.
|| Purdue University.
⊥ Heinrich-Heine University.

Table 1. ED_{50} Values (μg/mL) of *Delisea pulchra* Derived Natural Products Observed with Cancer Cell Lines in Culture

compound	BCA1[a]	HT-1080	Lu1	Mel2	Col1	KB	KB−V1[b]	KB+V1[c]	P-388	A431	LNCaP	ZR-75-1	U-373
1	NT	NT	>20	NT	NT	2.4	4.1	7.1	NT	NT	12.9	7.9	NT
3	NT	NT	>20	NT	NT	>20	>20	>20	NT	NT	9.1	6.4	NT
4	NT	NT	>20	NT	NT	5.4	10.7	2.8	NT	NT	1.7	2.4	NT
5	NT	NT	>20	NT	NT	3.9	5.6	4.7	NT	NT	3.6	4.0	NT
6	NT	NT	>20	NT	NT	6.1	5.3	6.1	NT	NT	4.5	3.8	NT
7	NT	NT	>20	NT	NT	4.1	3.9	6.2	NT	NT	3.6	2.8	NT
8	NT	NT	>20	NT	NT	7.6	10.5	8.0	NT	NT	6.6	6.7	NT
9	NT	NT	1.7	NT	NT	0.8	2.1	1.0	NT	NT	0.5	1.6	NT
11	NT	NT	0.3	NT	NT	0.4	3.4	0.1	NT	NT	0.2	<0.1	NT
12	NT	NT	0.6	NT	NT	0.5	0.2	1.1	NT	NT	<0.1	0.3	NT
13	9.8	2.2	>20	5.3	>20	>20	>20	>20	>5	>20	7.3	10.2	10.0
14	NT	NT	1.3	NT	NT	0.4	4.1	0.3	NT	NT	<0.1	0.3	NT
16	NT	NT	1.5	NT	NT	0.1	3.6	0.2	NT	NT	2.0	<0.1	NT
17	NT	NT	1.0	NT	NT	0.4	1.2	1.4	NT	NT	3.0	0.4	NT
19	NT	NT	1.7	NT	NT	0.5	0.6	9.5	NT	NT	6.7	0.3	NT
20	NT	NT	1.1	NT	NT	0.3	0.5	3.5	NT	NT	2.1	<0.1	NT
21	6.4	>20	10.3	4.2	12.4	>20	>20	>20	>5	10.5	9.3	8.6	>20
23	>20	>20	>20	>20	>20	>20	>20	>20	>5	>20	>20	>20	>20
25	NT	NT	>20	NT	NT	6.9	5.0	5.8	NT	NT	6.9	5.3	NT

[a] Abbreviations of cell lines: BCA1 (human breast cancer), HT-1080 (human fibrosarcoma), Lu1 (human lung cancer), Mel2 (human melanoma), Col1 (human colon cancer), KB (human epidermoid carcinoma of the mouth), KB−V1 (vinblastine-resistant KB), P-388 (mouse lymphoid neoplasm), A431 (human epidermoid carcinoma), LNCap (hormone-dependent human prostate cancer), ZR-75-1 (hormone-dependent human breast cancer), U-373 (human glioblastoma). [b] (−VLB) without vinblastine. [c] (+VLB) with vinblastine. [d] NT = not tested.

Table 2. Antibacterial and Antifungal (Antimicrobial) Activities of *Delisea pulchra* Derived Natural Products

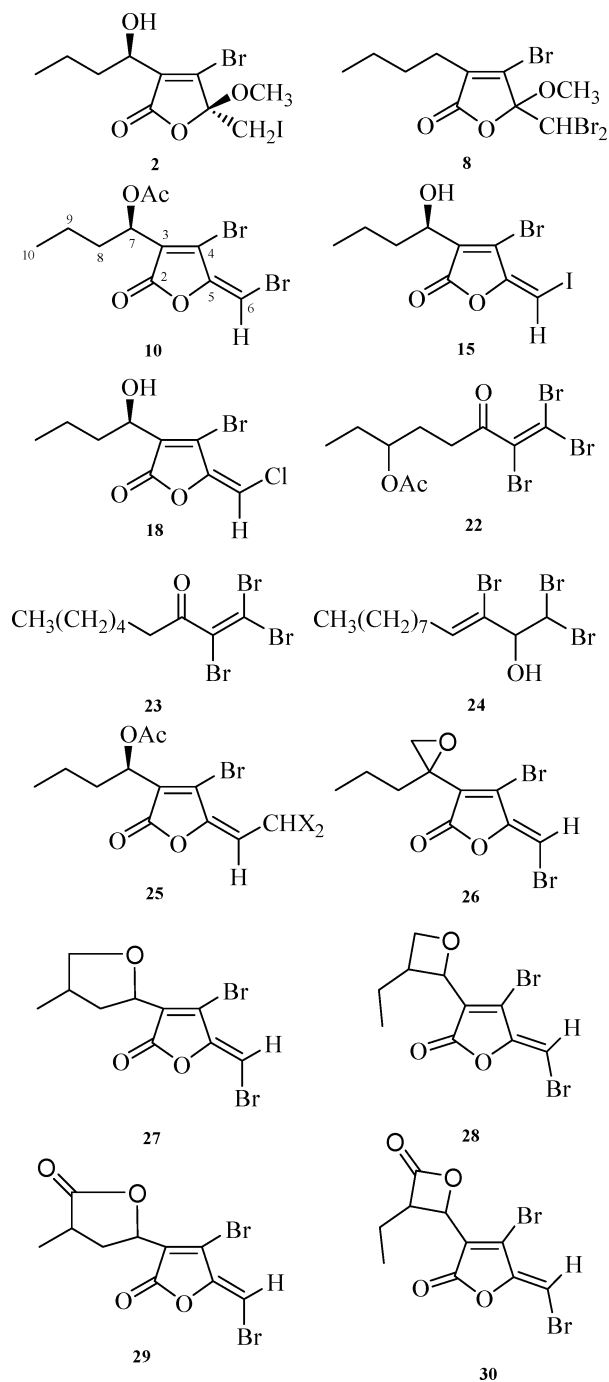| compound	*E. coli*[a]				*M. luteus*[a]				*B. subtilis*[a]				*P. oxalis*[b]				
	10 μg	5 μg	1 μg	0.1 μg	10 μg	5 μg	1 μg	0.1 μg	10 μg	5 μg	1 μg	0.1 μg	10 μg	5 μg	1 μg	0.1 μg	0.01 μg
1	−[c]	−	−	−	+	+	−	−	−	−	−	−	−	−	−	−	NT
2	+	+	−	−	+	+	−	−	+	+	−	−	14	16	10	−	NT
3	+	+	−	−	+	+	−	−	+	−	−	−	6	6	2	−	NT
4	−	−	−	−	+	+	+	−	−	−	−	−	8	6	3	−	NT
5	−	−	−	−	+	+	−	−	+	+	−	−	16	12	8	−	NT
6	−	−	−	−	−	−	−	−	−	−	−	−	9	8	4	−	NT
7	−	−	−	−	+	+	−	−	+	+	−	−	16	14	6	−	NT
8	+[d]	+	+	−	++	++	+	−	−	−	−	−	−	−	−	−	NT
9	+	−	−	−	++	++	+	−	++	++	++	NT	16	15	11	7	−
10	−	−	−	−	++	++	+	+	++	++	++	−	18	22	14	6	−
11	++	++	++	NT[f]	++	++	++	−	++	++	++	+	27	26	20	6	−
12	++	++	++	NT	++	++	++	−	++	++	++	+	28	31	21	6	−
13	+	−	−	−	++	++	+	−	+	−	−	NT	3	3	−	NT	NT
14	+	+	+	−	++	++	+	−	++	++	−	−	20	18	12	4	NT
16	+	+	−	−	++	++	+	+	++	++	++	−	17	21	9	6	−
17	++[e]	++	+	+	++	++	+	−	++	++	+	−	22	18	14	6	NT
19	+	+	−	−	++	++	++	+	++	++	++	NT	20	23	17	NT	4
20	+	+	−	−	+	+	+	+	++	++	++	NT	12	14	10	6	3
21	+	+	−	−	++	++	−	NT	++	++	−	NT	11	13	8	1	−
22	+	+	−	−	−	−	−	NT	+	+	−	NT	8	9	6	−	−
23	−	−	−	−	+	+	−	NT	−	−	−	NT	10	5	−	NT	NT
24	+	−	−	−	+	+	−	NT	+	+	−	NT	8	8	5	−	−
25	+	+	+	−	+	+	+	−	+	+	−	−	12[g]	10	6	4	NT

[a] Control was tetracycline-HCl, which was still active at 0.1 μg against *E. coli* and active at 1 μg against *B. subtilis* and *M. luteus* but inactive against the latter two at 0.1 μg. [b] Control was miconazole, which gave 3 and 5 mm inhibition zones at levels of 0.8 and 1.6 μg, respectively. [c] − = inactive; compound does not inhibit microorganism growth in any way. [d] + = active; compound inhibits growth of microorganism in region on TLC plate where it was spotted. [e] ++ = very active; compound inhibits growth of microorganism in region on TLC plate where it was spotted and for at least another 5 mm. [f] NT = not tested. [g] Number indicates radius of zone of inhibition in mm around point where compound was spotted on TLC plate.

stronger inhibition against Gram-positive bacteria. Nearly all of the compounds showed at least moderate in vitro activity against the Gram-positive bacteria *B. subtilis* and *M. luteus* at the highest levels tested, 10 and 5 μg (Table 2). The most active compounds were further tested at 1.0 and 0.1 μg, and four furanones (**10**, **16**, **19**, **20**) were active against *M. luteus* at 0.1 μg, while two other compounds (**11**, **12**) were active against *B. subtilis* at 0.1 μg. This activity is greater than that of the positive control (tetracycline-HCl), highlighting the potent activity of these compounds against Gram-positive bacteria.

In contrast to the Gram-positive bacteria the growth of the Gram-negative bacterium *E. coli* was inhibited by approximately half of the compounds at the 10 and 5 μg levels. Fewer compounds (**8**, **11**, **12**, **14**, **17**, **25**) were active at 1.0 μg, and only one compound

(**17**) inhibited the growth of *E. coli* at a concentration of 0.1 μg, that is, equivalent to the positive control (tetracycline-HCl).

The activity of the isolated compounds was also very strong against the fungus *P. oxalis*. Activity was detected for all but two compounds (**1**, **8**) at the highest concentration (10 μg). Ten compounds (**9**, **10**−**12**, **14**, **16**, **17**, **20**, **21**, and **25**) maintained strong activity at 0.1 μg, while two compounds, **19** and **20**, demonstrated strong antifungal effects at a concentration of 0.01 μg. This activity is equivalent to that of the positive control miconazole when tested at a concentration approximately 2 orders of magnitude higher than the furanones (0.8 μg, 3 mm inhibition zone). This demonstrates the potency of these compounds as antifungal agents and is consistent with the earlier study of using a restricted subset of furanones.[2]

Table 3. Antimalarial Activity of *Delisea pulchra* Derived Natural Products Determined with *P. falciparum* Clones

compound	KB cells IC$_{50}$	clone D6[a] IC$_{50}$[b]	SI[c]	clone W2[a] IC$_{50}$	SI
6	6.1	3.8	~2	>10	−
7	4.1	5.0	~1	>10	−
14	0.4	6.8	<1	>10	−
16	0.1	4.6	<1	>10	−
17	0.4	5.9	<1	>10	−
19	0.5	2.8	<1	>10	−
20	0.3	2.2	<1	9.1	<1
chloroquine	17.4	0.003	6210	0.033	530
quinine	>20	0.011	>1830	0.029	>700
mefloquine	3.5	0.005	710	0.001	4380
artemisinin	>20	0.001	>18 200	0.006	>3280

[a] Clone D6: chloroquine sensitive, clone W2: chloroquine resistant. [b] IC$_{50}$ values in μg/mL. [c] Selectivity index (SI) is defined as the ratio of antimalarial over cytotoxicity activity. Compounds **1**, **3**−**5**, **8**, **9**, **11**−**13**, **21**, **23**, and **25** were also tested and found to be inactive (at 10 μg/mL parasite viability was >50%).

Table 4. Tyrosine Kinase (TK) Inhibition Activity of *Delisea pulchra* Derived Natural Products

compound	% residual enzyme activity[a]
2	77.2
3	55.7
5	86.0
6	87.5
7	22.7
11	3.4
14	4.2
15	5.8
17	1.9
18	1.6
19	4.5
20	1.9
22	31.7

[a] Test substance concentration is 200 μg/mL.

Table 5. Inhibition of Interleukin-1 (IL-1) Induction and Protein Biosynthesis by *Delisea pulchra* Derived Natural Products

compound	IC$_{50}$ IL-1 (μM)	IC$_{50}$ protein biosynthesis (μM)
9	1.3	3.0
11	0.6	1.5
21	1.8	3.0
22	2.0	2.0
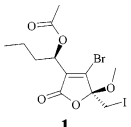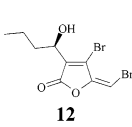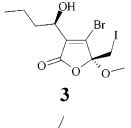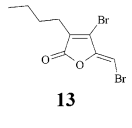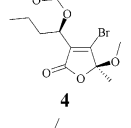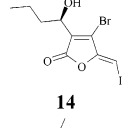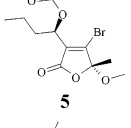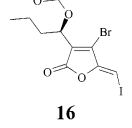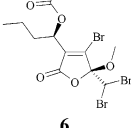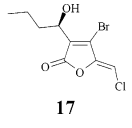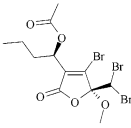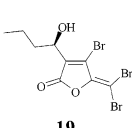
Of these, seven were active (**11**, **14**, **15**, and **17**−**20**, see Table 4), but not at a level warranting determination of IC$_{50}$ values.[21]

Interleukin-1 Inhibition Activity and Protein Biosynthesis. The production of interleukin-1 was inhibited by all four compounds used in this assay (**9**, **11**, **21**, and **22**), all with IC$_{50}$'s ≤ 2.0 μM (see Table 5). However, this activity was unspecific, as the compounds also inhibited protein biosynthesis at similar concentrations (see Table 5).[23]

Antitubercular Activity. The three compounds tested (**1**, **9**, and **11**) for their abilities to inhibit *Mycobacterium tuberculosis* and *M. avium* were ineffective at 128 μg/mL (~350 μM).[24]

Pseudoreceptor Modeling. A quasi-atomistic receptor modeling strategy aimed at creating a 3D pseudoreceptor envelope accommodating the molecular ensemble of interest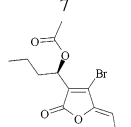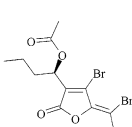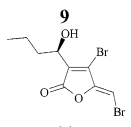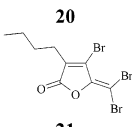 was applied to elucidate the differential cytotoxicity (anticancer activity) toward KB−V1 (Vinblastine-resistant KB cells) cells, in the absence of vinblastine, for 16 furanones (see Table 6). This study simultaneously provides detailed structure−activity relationships for these 16 biologically active compounds.[25] The concept of quasi-atomistic receptor surface surrogates was used in a pseudoreceptor modeling study,[26] in which virtual particles with associated physicochemical properties, such as hydrophobicity, partial charge, electrostatic potential, and hydrogen-bonding propensities, were employed for

In Vitro Antimalarial Activity (or Antiplasmodial Activity). Nineteen compounds were tested for their antiplasmodial activity toward two clones of *Plasmodium falciparum* (Table 3). Of these, seven (**6**, **7**, **14**, **16**, **17**, **19**, and **20**) exhibited weak antiplasmodial activity but with no selectivity.[20] The remainder were all classified as inactive, with an IC$_{50}$ > 1000 ng/mL (>1 μM).[20]

HIV-1 RT Inhibition Activity. The HIV-1 RT inhibition activity was assessed for 16 compounds (**1**, **3**−**9**, **11**, **12**, **14**, **16**, **17**, **19**, **20**, and **25**). All compounds were inactive at 200 μg/mL (~700 μM).[21]

Protein Kinase C Inhibition Activity. Six compounds (**9**, **11**, and **21**−**24**) were tested for the inhibition of the enzyme protein kinase C. The two most active compounds, **9** and **11**, had IC$_{50}$'s of 67 and 76 μM, respectively. The remaining compounds had IC$_{50}$'s ≥ 200 μM and were inactive.[22]

Tyrosine Kinase Inhibition Activity. Thirteen compounds were assayed for tyrosine kinase inhibition at 200 μg/mL (~700 μM).

Table 6. Compounds Used for Pseudoreceptor Modeling and Their Associated Biological Activities

Compound	CDS[a] template	ED$_{50}$ [µM][b]	Set Type[c]	Compound	CSD[a] template	ED$_{50}$ [µM][b]	Set Type[c]
1	ZAQTOA[d]	9.17	Test	**12**	GAJWET[f]	0.61	Training
3	TAGGIR[e]	>49.38	Training	**13**	GAJWET[f]	>64.52	Test
4	ZAQTOA[d]	33.32	Training	**14**	GAJWET[f]	10.99	Training
5	TAGGIR[e]	17.44	Training	**16**	GAJWET[f]	8.67	Training
6	ZAQTOA[d]	11.07	Training	**17**	GAJWET[f]	4.26	Test
7	TAGGIR[e]	8.14	Training	**19**	GAJWET[f]	1.48	Test
9	GAJWET[f]	5.71	Training	**20**	GAJWET[f]	1.12	Training
11	GAJWET[f]	10.43	Test	**21**	GAJWET[f]	>54.43	Training

[a] CSD: Cambridge Structural Database. [b] ED$_{50}$ values of *D. pulchra* derived natural products observed with cancer cell lines (KB−V1) in culture. [c] Set type refers to whether the molecule was used for receptor surface construction (training) or for testing its validity (test). [d] CSD entry code: ZAQTOA. [e] CSD entry code: TAGGIR. [f] CSD entry code: GAJWET.

the 16 closely related furanones, which have a well-differentiated in vitro activity profile on cancer cell lines (see Tables 1 and 6). Since the corresponding proteinogenic molecular target for this class of natural products is unknown, it is presumed that all compounds of the ensemble (i) bind to a common molecular target and (ii) share a comparable binding mode.

According to the method of Marengo and Todeschini for an unbiased selection of a structurally and topologically diverse training set based on the minimum-distance approach,[27] 11 compounds from the data set were chosen as a training set (**3**−**7**, **9**, **12**, **14**, **16**, **20**, **21**) in the model-building process. Molecules **1**, **11**, **13**, **17**, and **19** served as a test set for validation after model refinement (Table 6). Both 3D structure information on the investigated ligand molecules and their associated biological activities were translated into relative free energies of binding [$\Delta G = -RT \ln(\text{ED}_{50})$] and further corrected for desolvation effects (ΔG_{solv}), loss of conformational entropy ($T\Delta S$), and internal conformational strain (ΔE_{strain}).[28−30] After the definition of the training set, a primordial receptor surface was generated around the ligands. This preliminary envelope, consisting of 207 pseudoparticles with a radius of 0.8 Å, was subsequently employed as starting configuration for relaxation and adjustment to the topology of every ligand molecule. During this process every

surface particle was weakly restrained to the initial position represented by the mean receptor envelope. For the training set compounds an initial population of 200 receptor models was evolved for 5000 crossover cycles applying the genetic algorithm technology developed by Rogers and Hopfinger.[31]

The upper threshold value for the cross-validated q^2 was set to 0.9. The best individual model (model 145) within the ensemble of 200 generated models is characterized by a cross-validated $q^2 = 0.929$ and a classical r value for the linear regression analysis of 0.968. The five test set molecules were then evaluated in light of the generated pseudoreceptor models in order to validate the model family. The predictive power for the best receptor model that is expressed as the rms (root mean square) deviation of the experimental and predicted free energies of the ligand binding resulted in 0.197 kcal·mol^{-1} for the training set, corresponding to a mean uncertainty factor of 1.4 in the binding constant and 0.888 kcal·mol^{-1} for the test set, corresponding to a mean uncertainty factor of 4.6 in the binding constant, respectively. The details of the energetic analysis for all individual training and test set ligands are summarized in Table 7.

The largest individual deviation between predicted and experimental free energies of binding is observed for compound **13**

Table 7. Comparison of Experimental and Predicted Relative Free Energies (kcal·mol^{-1}) for the Best Model and the Average Model Taken over 200 Distinct Models

compound	$\Delta G°_{exp}{}^a$	$\Delta G°_{pred}{}^b$	$\Delta\Delta G°_{exp-pred}{}^c$	factor in k^d
Best Model				
Training Set				
3	−5.771	−5.818	−0.047	1.1
4	−6.000	−5.921	0.079	1.1
5	−6.376	−6.159	0.217	1.5
6	−6.641	−6.891	−0.250	1.5
7	−6.820	−6.611	0.209	1.4
9	−7.026	−6.747	0.279	1.6
12	−8.328	−8.106	0.222	1.5
14	−6.645	−6.905	−0.260	1.6
16	−6.783	−6.959	−0.176	1.4
20	−7.974	−8.084	−0.110	1.2
21	−5.747	−5.912	−0.165	1.3
Test Set				
1	−6.750	−5.816	0.934	5.0
11	−6.675	−6.688	−0.013	1.0
13	−5.615	−4.295	1.320	9.7
17	−7.197	−6.350	0.847	4.3
19	−7.812	−8.592	−0.780	3.8
Average over 200 Models				
Training Set				
3	−5.771	−5.817	−0.046	1.1
4	−6.000	−5.823	0.177	1.4
5	−6.376	−6.241	0.135	1.3
6	−6.641	−6.774	−0.133	1.3
7	−6.820	−6.688	0.132	1.3
9	−7.026	−6.720	0.306	1.7
12	−8.328	−7.984	0.344	1.8
14	−6.645	−6.745	−0.100	1.2
16	−6.783	−7.083	−0.300	1.7
20	−7.974	−8.127	−0.153	1.3
21	−5.747	−6.111	−0.364	1.9
Test Set				
1	−6.750	−5.864	0.886	4.6
11	−6.675	−6.558	0.117	1.2
13	−5.615	−4.487	1.128	6.9
17	−7.197	−6.265	0.932	5.0
19	−7.812	−8.434	−0.622	2.9

^{a} Experimental free energy of ligand binding. ^{b} Predicted free energy of ligand binding. ^{c} Difference between experimental and predicted free energies of ligand binding. ^{d} Uncertainty factor in the ED$_{50}$ value.

($\Delta\Delta G°_{exp-pred}$ = 1.320 kcal·mol^{-1}), which corresponds to an uncertainty factor of 9.7 in the binding constant (Table 7). When analyzing the average over the entire ensemble of the 200 receptor models, a cross-validated q^2 of 0.884 together with the classical r value for linear regression of 0.947 is obtained (Figure 1). The rms deviation of predicted and experimental free energies of ligand binding is calculated to be 0.225 kcal·mol^{-1} (uncertainty factor of 1.5 in the binding constant) for the training set and 0.816 kcal·mol^{-1} (uncertainty factor of 4.1 in the binding constant) for the test set. Again, compound **13** shows with $\Delta\Delta G°_{exp-pred}$ = 1.128 kcal·mol^{-1} the largest deviation energy, corresponding to an uncertainty factor of less than 7 in the binding constant. In Figure 2 the averaged model accommodating the superimposed test and training set compounds is depicted. The 207 virtual particles form a coherent pseudoreceptor surface with associated physicochemical properties that account for mutual physicochemical complementarity. The fact that the construction of the pseudoreceptor family for the furanones with anticancer activities yielded a model that has a relatively high predictive power (q^2 = 0.929; r = 0.968) supports the assumption that the molecules described in this study are targeted against a common receptor, probably a protein, and utilize a similar mode of binding.

With 193 out of 207 pseudoreceptor particles being hydrophobic and/or uncharged, the generated hypothetical binding surface reflects the overall lipophilic nature of the potential ligand compounds (Figure 2). Polar groups within side-chains, i.e., acetoxyl or
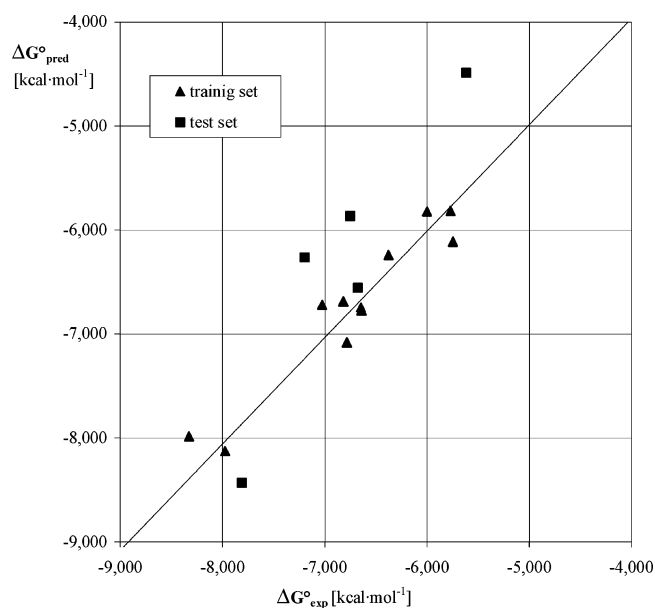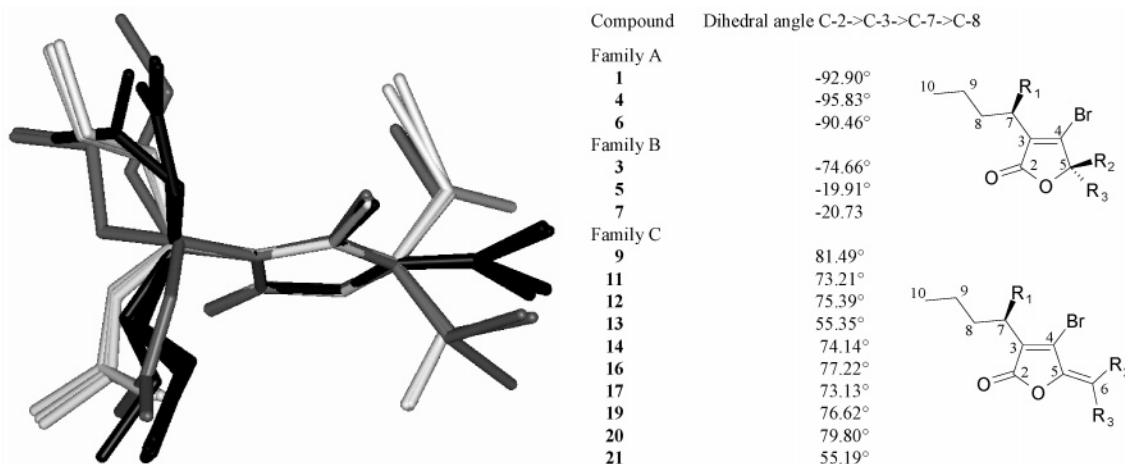

Figure 1. Correlation between $\Delta G°_{exp}$ and $\Delta G°_{pred}$ for the averaged pseudoreceptor model, characterized by a cross-validated q^2 of 0.884 and a classical r value for linear regression of 0.947.

hydroxyl, may function as hydrogen-bond acceptors or hydrogen-bond donors, respectively. A correlation of structure and activity in terms of the constitution of the involved molecules seems to be rather speculative, as active molecules are found in the group of furanones with an sp^3-configured C-5 atom, e.g., compounds **1** and **7**, both ranging in the single digit molar range, as well as in the group of compounds exhibiting an exocyclic double bond in that position, e.g., the most active compound (**12**) showing activity in the submicromolar range (0.61 μM). Considering R$_1$, the SAR shows a slight preference for the acetylated derivative to be the more active compound, which is demonstrated by the biological profile of compounds **19** (1.48 μM) and **20** (1.12 μM). In general, the acetylation seems to result in a slightly enhanced activity, which is also demonstrated by the structural pairs **9/11** (5.71 μM/10.43 μM) and **14/16** (10.99 μM/8.67 μM) for the acetylated/nonacetylated compound, respectively. On the other hand the lack of functionality at that position (**13**, **21**) leads to a loss in activity. With respect to the configuration of C-5, a tendency for an R-configured C-5 atom seems to be a prerequisite for enhanced activity compared to the S-isomers. Compound pair **4/5** (33.32 μM/17.44 μM), as well as **6/7** (11.07 μM/8.14 μM), show the R-configured isomer to be the slightly more active compound. In the series of furanones with an exocyclic double bond the activity profile of compounds **11** and **12** accounts for an E-configured exocyclic double bond as prerequisite for higher activity. While the Z-configured isomer, **11**, shows activity within the double-digit range (10.43 μM), compound **12** exhibits the highest activity within the entire ensemble (0.61 μM).

Although no dramatic changes within activity could be observed for the ensemble of 16 molecules, it was possible to obtain a differentiated 3D QSAR pursuing a pseudoreceptor modeling approach with the program Quasar. To prove the validity of the generated pseudoreceptor model, a scramble test was performed, which resulted in a classical q^2 value of −0.211 and an r value of −0.083, demonstrating that the obtained pseudoreceptor model for the ensemble is not generated accidentally. Within the training set the accuracy of predicting the biological activity is shown by low uncertainty factors ranging from 1.1 to 1.6 in the best model and 1.1 to 1.9 within the averaged model. The highest uncertainty factor is produced by compound **13**, a fact that may be explained by the absence of functionality at R$_1$, even though the corresponding compound in the training set (**21**) could be well predicted.
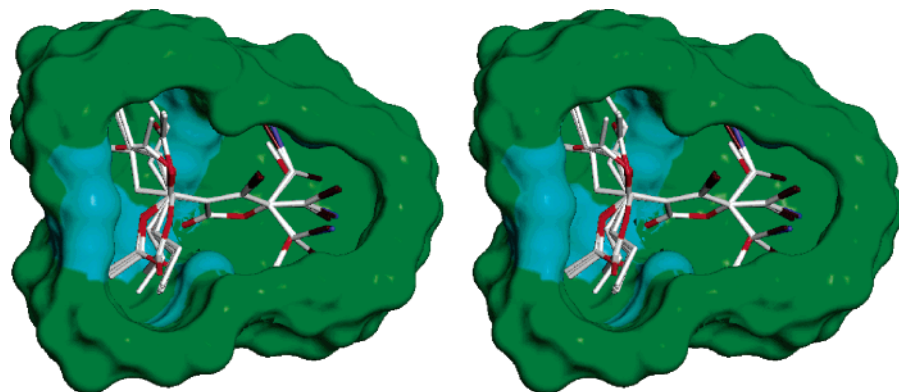
Figure 2. Stereoview of the superimposed training and test set molecules within the constructed pseudoreceptor surface. The surface engages the layer of virtual particles between the inner and outer surfaces. Areas populated by hydrophobic virtual particles are shown in green, while spatial areas with positively and negatively charged properties together with hydrogen-bond donor capacities are colored cyan.

| Compound	Dihedral angle C-2->C-3->C-7->C-8
Family A	
1	-92.90°
4	-95.83°
6	-90.46°
Family B	
3	-74.66°
5	-19.91°
7	-20.73
Family C	
9	81.49°
11	73.21°
12	75.39°
13	55.35°
14	74.14°
16	77.22°
17	73.13°
19	76.62°
20	79.80°
21	55.19°

Figure 3. Superposition of the furanones used for pseudoreceptor modeling (left). According to their flexibility around the C-3→C-7 bond, three families differing in side-chain conformation described by the dihedral angle C-2→C-3→C-7→C8 are formed (right). Family A is composed of compounds **1**, **4**, and **6** (white), family B of compounds **3**, **5**, and **7** (gray), and family C of compounds **9**, **11**, **12**, **13**, **14**, **16**, **17**, **19**, **20**, and **21** (black).

Prior to discussions of potential interactions of functional groups of the ligand molecules and the created receptor surface composed of virtual particles with associated physicochemical properties, one has to consider flexibility within the ligand compounds. To take account of different possible side-chain conformations, especially concerning the torsion around the bond between C-3 and C-7, which is described by the dihedral angle of C-2→C-3→C-7→C-8, different substituted furanones were chosen from CSD (Cambridge Structure Database)[34,35] as template molecules for the construction of the training and test set compounds (Table 6, Figure 3). While compounds belonging to family A are characterized by a dihedral angle of approximately −90°, those in family B display a dihedral angle between −20° and −75°. In contrast to compounds belonging to families A and B, those of family C exhibit an exocyclic double bond (C-5/C-6). According to that constitutional difference, a further template was chosen from CSD, compared to families A and B compounds, which resulted in dihedral angles ranging from +55° to +80°. Consequently, functional groups within the side-chain R_1 are oriented in the "southwestern" portion within the pseudoreceptor cavity, while for compounds **9−21** the side-chain R_1 protrudes into the "northwestern" portion of the pseudoreceptor envelope (Figures 2 and 3). Correspondingly, the carbonyl-oxygen of the acetoxyl group within R_1 in compounds **1**, **4**, and **6** interacts with virtual particles (VPs) 56 and 58 (Figure 4). Both particles are characterized as H-bond donors at distances of approximately 2.3 Å or approximately 2.7 Å, respectively. The corresponding interaction for compounds **5** and **7** between the carbonyl oxygen and VPs 68 and 69 is found at approximately 2.3 Å and approximately 2.5 Å,

respectively. Hence, those VPs show positive salt-bridge characteristics. While the acetoxyl group of compound **9** is oriented toward the "northwest" part within the pseudoreceptor envelope, the acetoxyl groups of compounds **16** and **20** are positioned toward the "northeast" compartment. Interaction points are disposed by the VPs 46 and 66 for compound **9** and VPs 153, 178, and 180 for compounds **16** and **20**. The distance between the carbonyl oxygen of **9** and VP 46 is measured at 2.9 Å, and the distance to VP 66 is 2.6 Å. The corresponding interaction between the carbonyl oxygen of the acetoxyl group in compounds **16** and **20** is found at 2.6 and 2.7 Å to VP 153, approximately 2.5 Å to VP 178, and 2.7 or 2.9 Å to VP 180, respectively. The hydroxyl functionality (R_1) in compounds **11**, **12**, **14**, **17**, and **19** serves as a hydrogen-bond donor to the acceptor particle 115 at a distance of approximately 1.5 Å. As all compounds are superimposed with respect to the furanone ring, the general interaction point of the lactone carbonyl oxygen is found to be the same virtual particle, VP 52, at a distance of about 2.3 Å.

Concluding, the molecular modeling study, i.e., the pseudoreceptor modeling approach applying a 3D QSAR technique, results in a correlation of experimental and predicted free ligand binding energies characterized by a high cross-validated q^2 value (0.88, averaged model). The generated overall hydrophobic pseudoreceptor surface accounts for the mainly hydrophobic nature of the superimposed ensemble of 16 selected furanone entities. Corresponding interactions between functional groups within the ligands and pseudoreceptor particles with associated physicochemical properties account for the complementarity generated by the receptor envelope.
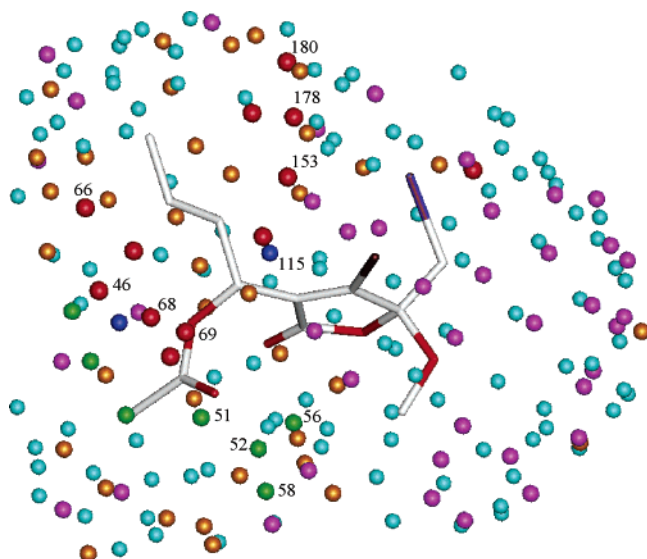
Figure 4. Averaged pseudoreceptor model composed of virtual particles accommodating compound **1**. The distribution for the 207 various virtual particles (VPs) is as follows: 7 uncharged H-bond donor VPs (green), 37 slightly positively charged (+0.1) hydrophobic VPs (orange), 40 slightly negatively charged (−0.1) hydrophobic VPs (pink), 109 uncharged hydrophobic VPs (cyan), and 12 positively charged (+0.25) VPs (red) as well as 2 negatively charged (−0.25) VPs (blue). Selected VPs that are interacting with ligand entities are numbered.

The analysis of SAR suggests that (i) acetylation within side-chain R$_1$, (ii) *R*-configuration of C-5 within the sp³-configured series of furanones, and (iii) an *E*-configured double bond within the furanone series with the exocyclic double bond might be crucial determinants for the observed activities.

Structure−Activity Relationships. Of the 25 *D. pulchra* compounds tested in this study, all compounds, including linear structures, exhibited biological activity in at least one of the test systems employed. The similarity of the majority of the structures as furanones provides an opportunity to analyze for any structure−activity relationships these compounds may show in the assay systems.

In the cytotoxicity assays (Table 1) all of the furanones had either moderate (1−8 μg/mL) or significant activity (<1 μg/mL) in at least one of the employed cell lines. The only compound to show no activity was the one acyclic compound tested (**23**). From these results it may reasonably be concluded that the lactone moiety is responsible, at least to some extent, for the observed activity. It is also evident from the data in Table 1 that the compounds having the $\Delta^{5,6}$ double bond (e.g., **9**, **11**, and **14**) are more active than those without it (e.g., **1**, **3**, and **4**). Further, the presence of an acetoxyl or hydroxyl function at C-7 (e.g., **9**, **11**, and **14**) also enhances the activity of the molecule relative to those without this functionality (e.g., **13** and **21**).

These structure−activity relationships also hold true for the antimicrobial, antifungal, and tyrosine kinase inhibition activity. The most active metabolites in the antibacterial assays were **11** and **12** against Gram-negative and **11**, **12**, **19**, and **20** against Gram-positive. Similarly for the antifungal activity, compounds **19** and **20** had the most pronounced effects, with **11** and **12**, and a number of other compounds (**9**, **10**, **14**, **16**, **17**, **20**, **21**, **25**), an order of magnitude less active. In the tyrosine kinase inhibition activity seven compounds (**11**, **14**, **15**, **17−20**), of the 13 tested, inhibited this enzyme to 96% of its activity or greater at 200 μg/mL.

In the antimalarial testing, even though less than half of the substances were tested, a trend is discernible. Compounds **19** and **20** had the best activity out of the seven compounds (**6**, **7**, **14**, **16**, **17**, **19**, **20**) that showed activity at lower than 7 μg/mL. Aside from

the data for acyclic **23**, the only two other compounds that are inactive are those that lack a functionality at C-7, **13** and **21**. It should also be noted that these compounds were inactive in many of the cytotoxicity assays as well, indicating the functionality (OH or OAc) at C-7 to be an important prerequisite for activity. Although only six compounds were tested for PKC inhibition activity, the results obtained support the previous structure−activity correlations.

The results of this study concur with other data reported for secondary metabolites from *D. pulchra* in independent test systems.[2] Although previous studies have used a much narrower range of compounds, the trends in structure−activity relationships are the same. In a study on the effects of furanones on the settlement of fouling organisms,[10] the presence of an acetoxyl or hydroxyl function at C-7 increased the activity of these compounds relative to those without this functionality. This structure−activity relationship was consistent for tests against a marine bacterium and the epiphytic alga *Ulva* sp.[10] Mechanistic assays to determine the activity of furanones as inhibitors of AHL quorum sensing systems in Gram-negative bacteria have also demonstrated the same trend.[34] Furanones with an OH or OAc at C-7 are significantly more active in the inhibition of AHL regulated bioluminescence and have significantly stronger displacement of radiolabeled native AHL signals (³H-OHHL) than the equivalent furanone lacking a functional group (OH or OAc) at C-7.[34] Therefore, a consistent pattern in the structure−activity relationship of these compounds is found in whole organism prokaryote- and eukaryote-based assays and in molecular-based mechanistic assays.

Conclusions

Of the compounds tested and modeled in the current study, **11** and **12**, closely followed by **19** and **20**, are the most active in the applied test systems. It might be reasonably concluded that for a molecule to be active in the test systems applied in this study it must have structural and the implied physiochemical features (e.g., electron density maps) in common with this group. If the basic framework of compound **11** is taken as a basis for activity, it is clear that within this class of compound an OH function (sometimes an OAc; assay dependent) at C-7 and bulky electron-rich groups at C-6 are essential for the measured activities. As these molecules are rather small and somewhat rigid and their activities so well defined, it seems unlikely that their observed activities could be greatly enhanced by altering the functionalities at C-4 and C-6. There does however seem to be a good chance to improve activity, and possibly selectivity, by modifying the basic framework in the C-7 region of the molecule. Possible obvious modifications would be ones that introduce groups similar in physical and chemical properties to the OH and OAc functionalities already found at this location and apparently essential for the observed activity. A number of possibilities might be the ethers represented by theoretical compounds **26−28** or the lactones represented by compounds **29−30**. Evident from the research undertaken to date is the fact that the natural compounds discussed in this work, if not directly useful in a given application where they have been found to have activity, will certainly be extremely useful as lead structures for further medicinal chemistry.

Experimental Section

General Experimental Procedures. As previously described.[35]

Materials. Compounds **1−25** were derived from previous studies made with *D. pulchra*.[4,5] Remaining materials are as previously described.[35]

Bioassays. The cytotoxic activity of 19 compounds (**1**, **3−9**, **11−14**, **16**, **17**, **19−21**, **23**, and **25**) was evaluated against a panel of 12 different cell lines.[17] Antimicrobial activity of *Delisea* metabolites was established using direct bioautographic assays as described.[18] Compounds were spotted on TLC plates, the solvent was evaporated, and the plates were used directly for the antimicrobial testing. Antimalarial assays were performed in vitro with *Plasmodium falciparum* clones

D6 (chloroquine-sensitive) and W2 (chloroquine-resistant).[20] Inhibition of reverse transcriptase activity of human immunodeficiency virus type-1 (RT HIV-1) was assayed in an ELISA-based system.[21] Inhibition of protein kinase C (PKC) was measured according to the methods employed by Meyer et al.[22] Inhibition of tyrosine kinase (TK p56*lck*) was assessed as described by Kirsch et al.[21] Inhibition of interleukin-1 and protein biosynthesis was investigated according to the methods of Rordorf-Adam et al.[23] Activity against *Mycobacterium tuberculosis* and *M. avium* was established according to the protocol described by Collins and Franzblau.[24]

Pseudoreceptor Modeling. All simulations were performed on a Silicon Graphics Indigo 2 workstation (R10000). The program IN-SIGHT II, version 98.0,[36] was used for model-building procedures and as graphical interface. For the purpose of this study, 16 furanones were selected. All of these furanones possess a common underlying framework, which corroborates the working hypothesis that these compounds address a common receptor-type target molecule and utilize a similar binding mode. This hypothesis is the basic assumption underlying all types of comparative molecular modeling approaches such as 3D QSAR and pseudoreceptor modeling techniques. According to this assumption, a molecular superposition of the 3D structures of the selected molecules, reflecting the common binding mode for the core structure (lactone ring), should enable the steric and physico-chemical characteristics responsible for the distinctive biological activities to be deduced. To generate the superimposed ensemble of compounds, the experimentally derived 3D structures of three template molecules were retrieved from the Cambridge Structure Database (CSD).[32,33] All compounds were manually constructed according to those template structures of closely related compounds (for details see Table 6) using the DISCOVER simulation package implemented in INSIGHT II. All compounds were then submitted to an energy minimization over 100 steps using the steepest descent algorithm within cvff (consistent valence force field), except for I-containing ligands, which were minimized under the same conditions within the force field cff91. All compounds were then subjected to an energy minimization using the AM1 Hamiltonian within MOPAC 6.0.[37] The atomic potential charge model (ESP charges) was obtained by using MOPAC 6.0 also. The individually geometry-optimized compounds were overlaid following an atom-based rigid body superposition. Within the subsequent pseudoreceptor modeling approach the ligands were kept fixed while the mean envelope was adjusted to the superimposed ligands by minimization within the software package PrGen 2.1.[38,39] The initial alignment of the 16 furanones served as input data for the quasi-atomistic receptor modeling approach. The superimposed ensemble of compounds was subjected to the program Quasar,[26] version 1.6, as implemented on the PrGen 2.1 platform. Quasar can be used to engage biologically active ligand molecules in specific intermolecular interactions with a sterically complementary receptor surface, to mimic macromolecular environments of low molecular weight compounds in their target-bound state. Quasar generates a family of receptor surface models in light of molecular structures and biological activities of the ligand set by means of a genetic algorithm combined with cross-validation. This approach was discussed in more detail previously.[35]

References and Notes

(1) Bonin, D. R.; Hawkes, M. W. *N. Z. J. Bot.* **1988**, *26*, 619−632.
(2) Reichelt, J. L.; Borowitzka, M. A. *Hydrobiologia* **1984**, *116/117*, 158−168.
(3) Kazlauskas, R.; Murphy, P. T.; Quinn, R. J.; Wells, R. J. *Tetrahedron Lett.* **1977**, *1*, 37−40.
(4) de Nys, R.; Coll, J. C.; Bowden, B. F. *Aust. J. Chem.* **1992**, *45*, 1625−1632.
(5) de Nys, R.; Wright, A. D.; Konig, G. M.; Sticher, O. *Tetrahedron* **1993**, *49*, 11213−11220.
(6) Maximilien, R.; de Nys, R.; Holmström, C.; Gram, L.; Givskov, M.; Crass, K.; Kjelleberg, S.; Steinberg, P. D. *Aquat. Microb. Ecol.* **1998**, *15*, 233−246.
(7) Wright, J. T.; de Nys, R.; Poore, A. G. B.; Steinberg, P. D. *Ecology* **2004**, *85*, 2946−2959.
(8) de Nys, R.; Steinberg, P. D.; Rogers, C. R.; Charlton, T. S.; Duncan, M. W. *Mar. Ecol. Prog. Ser.* **1996**, *130*, 135−146.
(9) de Nys, R.; Dworjanyn, S. A.; Steinberg, P. D. *Mar. Ecol. Prog. Ser.* **1998**, *162*, 79−87.
(10) de Nys, R.; Steinberg, P. D.; Willemsen, P.; Dworjanyn, S. A.; Gabelish, C. L.; King, R. J. *Biofouling* **1995**, *8*, 259−271.
(11) Givskov, M.; de Nys, R.; Manefield, M.; Gram, L.; Maximilien, R.; Eberl, L.; Molin, S.; Steinberg, P. D.; Kjelleberg, S. *J. Bacteriol.* **1996**, *178*, 6618−6622.
(12) Kjelleberg, S.; Steinberg, P. D.; Givskov, M.; Gram, L.; Manefield M.; de Nys, R. *Aquat. Microb. Ecol.* **1997**, *13*, 85−93.
(13) Ren, D.; Bedzyk, L. A.; Ye, R. W.; Thomas, S. M.; Wood, T. K. *Biotechnol. Bioeng.* **2004**, *88*, 630−642.
(14) Rice, S. A.; McDougald, D.; Kumar, N.; Kjelleberg, S. *Curr. Opin. Invest. Drugs* **2005**, *6*, 178−184.
(15) Hentzer, M.; Wu, H.; Anderson, J. B.; Riedel, K.; Rasmussen, T. B.; Bagge, N.; Kumar, N.; Schembri, M. A.; Song, Z.; Kristoffersen, P.; Manefield, M.; Costerton, J. W.; Molin, S.; Eberl, L.; Steinberg, P.; Kjelleberg, S.; Hoiby, N.; Givskov, M. *EMBO J.* **2003**, *22*, 3803−3815.
(16) Hentzer, M.; Riedel, K.; Rasmussen, T. B.; Heydorn, A.; Anderson, J. B.; Parsek, M. R.; Rice, S. A.; Eberl, L.; Molin, S.; Hoiby, N.; Kjelleberg, S.; Givskov, M. *Microbiology* **2002**, *148*, 87−102.
(17) Likhitwitayawuid, K.; Angerhofer, C. K.; Ruangrungsi, N.; Cordell, G. A.; Pezzuto, J. M. *J. Nat. Prod.* **1993**, *56*, 30−38.
(18) Hamburger, M. O.; Cordell, G. A. *J. Nat. Prod.* **1987**, *50*, 19−22.
(19) Baumgartner, B.; Erdelmeier, C. A. J.; Wright, A. D.; Rali, T.; Sticher, O. *Phytochemistry* **1990**, *29*, 3327−3330.
(20) Angerhofer, C. K.; Konig, G. M.; Wright, A. D.; Sticher, O.; Milhous, W. K.; Cordell, G. A.; Farnsworth, N. R.; Pezzuto, J. M. In *Advances in Natural Product Chemistry*; Atta-ur-Rahman, Ed.; Harwood Academic Publishers: Chur, Switzerland, 1992; pp 311−329.
(21) Kirsch, G.; Wright, A. D.; König, G. M. *J. Nat. Prod.* **2000**, *63*, 825−829.
(22) Meyer, T.; Regenass, U.; Fabbro, D.; Alter, E.; Rösel, J.; Müller, M.; Caravatti, G.; Matter, A. *Int. J. Cancer* **1989**, *43*, 851−856.
(23) Rordorf-Adam, C.; Geiger, T.; Henn, R.; Arnold, J.; Solf, R.; Wiesenberg, I.; Ferrini, P. G.; Vosbeck, K. *Agents Actions* **1994**, *43*, 53−59.
(24) Collins, L. S.; Franzblau, S. G. *Antimicrob. Agents Chemother.* **1997**, *41*, 1004−1009.
(25) Vedani, A.; Dobler, M.; Zbinden, P. *J. Am. Chem. Soc.* **1998**, *120*, 4471−4477.
(26) Gurrath, M.; Müller, G.; Höltje, H.-D. In *3D QSAR in Drug Design*; Kubinyi, H., Martin, J., Folkers, G., Eds.; Perspetives in Drug Discovery and Design; Kluwer Academic Publishers: Lancaster, 1998; 12/13/14, pp 135−157.
(27) Blaney, J. M.; Weiner, P. K.; Dearing, A.; Kollman, P. A.; Jorgensen, E. C.; Oatley, S. L.; Burridge, J. M.; Blake, J. F. *J. Am. Chem. Soc.* **1982**, *104*, 6424−6434.
(28) Marengo, E.; Todeschini, R. *Chemomet. Intell. Lab. Syst.* **1992**, *16*, 37−44.
(29) Still, W. C.; Temczyk, A.; Hawley, R. C.; Hendrickson, T. *J. Am. Chem. Soc.* **1990**, *112*, 6127−6129.
(30) Searle, M. S.; Williams, D. H. *J. Am. Chem. Soc.* **1992**, *114*, 10690−10697.
(31) Rogers, D.; Hopfinger, A. J. *J. Chem. Inf. Comput. Sci.* **1994**, *34*, 854−866.
(32) Allen, F. H.; Kennard, O. *Chem. Des. Autom. News* **1993**, *8*, 131−137.
(33) Bruno, I. J.; Cole, J. C.; Lommerse, P. M.; Rowland, R. S.; Taylor, R.; Verdonk, M. J.*Comput.-Aided Mol. Des.* **1997**, *11*−6, 525−537.
(34) Manefield, M.; de Nys, R.; Kumar, N.; Read, R.; Givskov, M.; Steinberg, P. D.; Kjelleberg, S. *Microbiology* **1999**, *145*, 283−291.
(35) Wright, A. D.; Wang, H.; Gurrath, M.; König, G. M.; Kocak, G.; Neumann, G.; Loria, P.; Foley, M.; Tilley, L. *J. Med. Chem.* **2001**, *44*, 873−885, and references therein.
(36) *INSIGHT II*, version 98.0; MSI: San Diego, CA, 1999.
(37) Steward, J. J. P. *J. Comput.-Aided Mol. Des.* **1990**, *4*, 1−105.
(38) Vedani, A.; Zbinden, P.; Snyder, J. P.; Greenidge, P. A. *J. Am. Chem. Soc.* **1995**, *117*, 4987−4994.
(39) Zbinden, P.; Dobler, M.; Folkers, G.; Vedani, A. *Quant. Struct.-Act. Relat.* **1998**, *17*, 122−130.